Leeghwaterstraat 44
2628 CA Delft
P.O. Box 6012
2600 JA Delft
The Netherlands

www.tno.nl

T +31 88 866 22 00
F +31 88 866 06 30

TNO report

TNO 2020 R12154 | 1

Geotechnical modelling guide: material models, parameter ranges, parameter estimation

Date	16 November 2020
Author(s)	J.P. Pruiksma
Copy no	
No. of copies	
Number of pages	35 (incl. appendices)
Number of appendices	1
Sponsor	
Project name	Kennisprogramma Natte Kunstwerken: Funderingsgedrag
Project number	060.32447/01.20.06

Contents

1 Introduction

This document contains a brief guide on geotechnical modelling. The focus is on Finite Element modelling (FEM), with some references given to literature that is known to give reasonable analytical results for a few applications (e.g. soil springs derivation). This document is targeted to engineers familiar with FEM but perhaps less familiar with constitutive models for soils or the estimation of soil parameters. The focus is on the material models that are more often used in TNO (elastodynamic, elasto-plastic with memory and the influence of pore pressures) rather than the more advanced models (cyclic behaviour, liquefaction, creep) which could be added in a subsequent study. This limitation allows use of well accepted soil material models and literature for parameter determination. In addition, most FEM packages are able to model these soil behaviours.

This document is structured as follows. Chapter 2 gives an overview of geotechnical modelling. It provides a summary of the types of material models, together with a discussion on the treatment of pore pressures and consolidation, stress initialization and the modelling of structural elements that interact with the soil. Some common definitions of geotechnical terms are discussed which can help avoiding trivial mistakes in FEM simulations. Chapter 3 discusses material behaviour in detail. The most realistic commonly available material modelling options are given, with alternatives for cases where the material models may not be available in a specific FEM package. Ranges of material parameters for different soil types are presented. If in soil parameter estimation values are found that are outside these ranges, it should trigger the engineer to investigate whether something is wrong. Chapter 4 details a procedure for soil parameter estimation from Cone Penetration Test (CPT) data for the material models discussed in Chapter 2. It is noted that currently this procedure makes use of the software CPT-iT3, but this software is based upon [Robertson 2009], [Robertson & Cabal 2009, 2015] whose equations can be implemented relatively easily (e.g. in Excel) in a subsequent project such that it can be used more widely in TNO.

2 Overview of geotechnical modelling

This Chapter presents an overview of soil material models of an increasing level of complexity, the handling of pore pressures and in-situ stress in FEM simulations, the importance of in-situ stress levels, and modelling of structural elements.

2.1 Levels of material models

The choice of soil material model depends on the type of geotechnical problem that needs to be solved. There are in a broad sense five levels of material models of increasing complexity:

1. Elastic models (Linear/Nonlinear).
2. Elasto-plastic models without memory. These depend on the stress state in the soil, but not on stress history.
3. Elasto-plastic models with unloading reloading (partial memory). These depend on stress state as well as stress history. This memory is usually described by the so called pre-consolidation pressure, the maximum isotropic effective stress reached in history.
4. Models describing creep, usually added on to models of type 3, because pre-consolidation pressure is an essential attribute of creep models
5. Models used for cyclic behavior. These come in different forms: hysteretic behavior needed for soil energy dissipation, models for cyclic soil densification and liquefaction models. Models of this kind often have more state parameters (memory) which can be in the form of (kinematic) hardening, nested yield surfaces with each of them tracked etc.

The more advanced a material model is, the more input parameters it tends to have. On the other hand these input parameters are generally not well known in the average engineering situation. It is common to choose a material model targeted to the application, one that is as complex as needed but not more.

Soil models in each of these 5 levels come in many flavours. Some target different types of soil (e.g. sand, silt, clay, peat), some are similar but have differences due to different implementations in the various FEM packages (e.g. Plaxis, Abaqus, Diana, LS-Dyna, Optum). In most cases input parameters can be converted between models of the same level, although the behaviour of the models still may differ in practice. In this document models up to level 3 are treated. This limitation allows use of well accepted soil material models and literature for parameter determination. In addition, most FEM packages are able to model these soil behaviours and conversion of parameters is often successful.

2.2 Pore pressures, drained/undrained behavior, consolidation

Soil is mostly a two-phase medium: The soil material and the material in the pores which is either water or air in most applications (although technically water has often a bit of air content, see [Verruijt 2012]). The presence of water, and (changing) pore pressures greatly affect the soil behavior. In FEM simulations, initial or in-situ pore pressures can be defined, which is discussed in the next section. Subsequently, assumptions need to be made about the behavior of pore pressures during the simulation. There are three modeling options generally used:

1. **Undrained**
   This is the short-term response of saturated soil, where loading of the soil and the time scale of interest is so fast that pore pressure changes due to deformation have not dissipated due to fluid flow.
2. **Consolidation**
   Compared to the previous case, the time scale is longer such that pore pressures that are buildup due to deformation are already partly dissipating due to fluid flow. In this case, a coupled deformation and pore fluid simulation method needs to be used.
3. **Drained**
   This is the case where excess pore pressures (relative to the initial in-situ pore pressures) are either not build up because of high permeability in sandy type soils, or layers which are dry and do not contain pore fluid. Another case is that the time scale is so long that any excess pore pressures can be considered dissipated and the history of buildup and dissipation of pore pressures is irrelevant to good approximation.

It is not always obvious what option to use in a simulation. Sometimes different options are necessary for different stages of a simulation. For example in dike or embankment construction it is common to use c*onsolidation*, because when a new soil layer is added pore pressures are buildup which affect stability. These pore pressures are dissipated with time and then another soil layer can be added. The timing and thickness of the added layer is carefully tuned using *consolidation* analysis. To evaluate an existing quay wall or foundation construction, on the other hand, it would make more sense to use the *drained* option when putting the FEM model trough the different stages of construction (e.g. initial state, installing sheet piles, excavation, installing anchors/stamps etc.) because pore pressures which were buildup up during different construction stages have long been dissipated. If one is interested in the stability of such construction for short term loadings (wave impact, water rise, etc.), in that case it is common to use the *undrained* option after the simulation model has been put through construction using *drained* option. This would hold only for the less permeable layers, such as clay. For sandy materials it is often sufficient to use the drained options throughout at least for non-dynamic loading. For shock waves sand can behave as *undrained*.

It is expected that most applications in TNO SR use a mix of *drained* and *undrained* behavior. And it is essential to evaluate based on time scale which option is to be used.

Note that in most FEM software, the *drained*, *undrained* and *consolidation* methods can be combined with all levels of material models as discussed above. For consolidation analyses the soil permeability (horizontal and vertical) needs to be specified as an additional input for the soil layers. Also these options may have different names in different FEM packages. For example, Abaqus does not explicitly mention these at all, but does have a coupled simulation option for consolidation. In Abaqus, the undrained or drained options are mostly a case of searching material models for options that allow incorporation of these principles. Where a mix of drained and undrained is required it is an advantage to use software that can accommodate this, e.g. DIANA, Plaxis, or Optum.

The *undrained* behaviour in some software can be modelled in different ways. For example in Plaxis there is an *Undrained A* and *Undrained B* option. One uses the soil parameters of the dry soil and computes the undrained effect based on those, the other option uses specifically effective undrained parameters. It depends on the application which is favourable.

2.3 In-situ stress and pore pressures

All soil material models discussed in section 2.1, with the exception of the elastic models, depend on the stress state in the soil. In FEM simulations it is necessary to initialize the stress state. This is usually carried out by estimating the vertical and horizontal stress in the soil, applying this to all elements and make an equilibrium with the external loads defined in the software. In this procedure the total stress (due to the soil + water weight), the pore pressures, and the effective stress (the stress acting in the soil skeleton itself) must be considered.

The Terzaghi principle states:

Total stress = effective stress + pore pressure

Only two of the three need to be specified and it depends on the software which two. The effective stress, since it’s due to the forces between soil grains, is mainly governing the soil material behavior such as plasticity and the ‘soil memory’. In FEM software packages, the in-situ vertical and horizontal stresses are often initialized and estimated in the following manner:

Vertical stress:
In most cases the total vertical stress is determined by the weight of the soil (+water in pores) column above a certain point in the FEM model. Then the pore pressure at that depth is subtracted from the total vertical stress to get the soil effective stress. Some FEM packages, such as Plaxis, can perform this automatically for the user based on water head definition.

The pore pressure is often derived from the phreatic water level using hydrostatic conditions. But sometimes this is imprecise. For example in an excavation pit, the water level in the non-excavated part of the soil is higher than in the excavated part where the water is often pumped out so the bottom of the pit is dry. If in the bottom of the pit the water level there is used, then there is a pore pressure discontinuity between the soil column just outside and just inside of the pit. Some software packages like Plaxis and Optum have features to interpolate between these field or carry out steady state flow calculations to have a more realistic initial pore pressure field. Other software, like Abaqus does not have this, but spatial fields of pressure can be defined or imported from a flow simulation. This requires more modeling effort.

Another typical case is that soil layers, in particular sandy aquifer layers have pore pressures that are controlled by other factors. For example a river may have a higher water level than is found in the soil behind a dike. And a sand layer found at a certain depth behind the dike may be in communication with the river. Then this sand layer would have a higher pore pressure than the one calculated based on phreatic water levels and hydrostatic conditions. Such cases can still be modelled by setting these types of layers to their specific phreatic levels. Discontinuities in pore pressure may still exist in these cases but tend to be less problematic numerically.

Horizontal stress

The horizontal effective stress in the soil is frequently defined in terms of a factor, denoted by K_0, on the vertical effective stress. The value of this factor depends on the over consolidation ratio (OCR) of the soil. For normally consolidated soil (OCR=1) the K_0 factor is relatively well established, and is denoted by $K_{0,nc}$ where nc stands for normally consolidated. An equation that is commonly used is:

$$K_{0,nc} = 1 - \sin(\varphi) \qquad (2.1)$$

with φ the soil friction angle as discussed in section 3.4. For over consolidated soil (OCR>1) different empirical relations exist and the K_0 factor is more uncertain. Some guidelines are given in section 3.5 where overconsolidated soil material models are treated and 4.3 for parameter estimation of the OCR. An equation commonly used for overconsolidated soils, see the Optum CE manual or [Mayne & Kulhawy 1982], is:

$$K_{0,oc} = K_{0,nc} OCR^{\sin\varphi} \qquad (2.2)$$

Where the oc stands for overconsolidation. For OCR=1 this reduces to the normally consolidated value.

Note 1: Overconsolidated soil is present where the load on the soil in the past was higher than in present. This can be artificial due to preloading, or natural. In the North East parts of the Netherlands, overconsolidation is often attributed to the ice age, where a thick ice layer is believed to have been present which has since disappeared. Soil classification from Cone Penetration Test data can help determine if soil is overconsolidated, see Chapter 4.

Note 2: that the above procedures are used in FEM packages to compute an initial estimate of in-situ stresses, but that, unless the soil layering and phreatic levels are uniform over the width of the model, there is in general no equilibrium of the soil stresses with the external gravity loading. It is necessary to have an initial *drained* simulation step to make this equilibrium. Most FEM packages, like Abaqus, DIANA, Plaxis, Optum, have this feature.

3 Soil material models and parameter ranges

This Chapter describes suitable soil material models for complexity levels 1-3 as discussed in section 2.1. Ranges of the input parameters are given for the different soil types: peats, clays, silts and sands. It is possible to find values outside these ranges, however they are not common or for materials not considered here such as coarse gravels.

This Chapter is organized as follows. First, soil density and permeability is considered. Density is a basic element for all soil material models, and permeability is a general parameter that can be used in combination with all material models when consolidation needs to be performed. Subsequently, the different options for elasticity are presented. Elasticity is also a component for more advanced models. Next, memory-less elasto-plasticity is discussed and finally the effect of loading history is introduced through a pre-consolidation pressure.

3.1 Soil Density

Soil can mostly be considered a two-phase (water+soil or air+soil) or three-phase (water+soil+air) medium. Since the density of air is negligible compared to that of water or soil material, to describe the density, mainly three quantities are necessary, γ_{sat} and γ_{unsat}. These are the unit weight of fully water saturated soil (below the phreatic level) and unsaturated soil (above the phreatic level). In addition, to compute effective stresses, the unit weight of water, γ_w, must also be specified. Typical ranges are given in the table below:

Parameter	description	Typical range*
γ_{sat}	Unit weight below phreatic level (saturated)	19 – 22.5 kN/m^3 for sands (higher values if very silty) 14 – 21 kN/m^3 for clays (lower=soft, higher=solid or sandy) 13 – 16 kN/m^3 for organic clays 10 – 13 kN/m^3 for peats
γ_{unsat}	Unit weight above phreatic level (unsaturated)	17 – 21 kN/m^3 for sands (higher values strong silty) 14 – 21 kN/m^3 for clays (lower=soft, higher=solid or sandy) 13 – 16 kN/m^3 for organic clays 10 – 13 kN/m^3 for peats
γ_w	Unit weight of water	9.81 kN/m^3 (fresh water) or 10.05 kN/m^3 (sea water)

**For more detailed ranges, see [NEN 9997-1+C2 table 2B] or [JCSS 2006]*

Note that the ranges given for γ_{unsat} are the unit weight of a natural moisture content soil, not the dry soil. For example, a common value for the porosity for sands is 0.4, the sand grain material itself has a unit weight of 26 kN/m^3. This results in a dry unit weight of (1-0.4) *26=15.6 kN/m^3, and a saturated unit weight of (1-0.4) *26 + 0.4*9.81=19.5 kN/m^3. This dry unit weight is considerably lower than the range of γ_{unsat} in the table for sands because it is uncommon to find completely dry sand in the Netherlands due to capillary forces and precipitation. Note that for clays and peats the range for γ_{unsat} is identical to the range of γ_{sat}. The water content in these materials does not deviate much from the saturated case in the field, because of their low permeability and type (clay itself tends to form bonds with water).

3.2 Soil hydraulic conductivity (permeability)

Dissipation of pore pressures is most often described in terms of a linear relation between flow rate and hydraulic gradient, the so called Darcy equation:

$$q = -k\frac{dh}{ds}$$

Here k is the hydraulic conductivity, dh is the difference in water head h in [m] over distance ds in [m], and q is the specific flow rate in m/s. Over an area A, the total flow is qA in [m^3/s].

The hydraulic conductivity k is an input parameter for flow simulation and consolidation analysis. In literature, hydraulic conductivity literature is sometimes called permeability, although some texts are specific that permeability is an intrinsic property and has the dimension of [m^2], while hydraulic conductivity is linked to a specific fluid. But not always. In Plaxis for example the hydraulic conductivity is called permeability and has dimensions of [m/d]. It is recommended to consult the manual of the FEM package being used for the precise definition of permeability/hydraulic conductivity. Also a check of the units of permeability is recommended (e.g. Plaxis by default uses m/d rather than m/s). Sometimes a horizontal and vertical hydraulic conductivity can be specified. This because soil tends to be deposited in layers and there is a natural anisotropy. Most of the time the distinction in engineering is not necessary and the same values are used for horizontal and vertical hydraulic conductivity. The table below from the OptumCE manual shows the ranges for typical soils:

<table>
<tr><td>K (cm/s)</td><td>10^{2}</td><td>10^{1}</td><td>1</td><td>10^{-1}</td><td>10^{-2}</td><td>10^{-3}</td><td>10^{-4}</td><td>10^{-5}</td><td>10^{-6}</td><td>10^{-7}</td><td>10^{-8}</td><td>10^{-9}</td><td>10^{-10}</td></tr>
<tr><td>K (m/day)</td><td>10^{5}</td><td>10^{4}</td><td>1,000</td><td>100</td><td>10</td><td>1</td><td>0.1</td><td>0.01</td><td>10^{-3}</td><td>10^{-4}</td><td>10^{-5}</td><td>10^{-6}</td><td>10^{-7}</td></tr>
<tr><td></td><td colspan="4">Permeable</td><td colspan="4">Semi-Permeable</td><td colspan="5">Impermeable</td></tr>
<tr><td>Unconsolidated Sand & Gravel</td><td colspan="2">Gravel</td><td colspan="3">Well Sorted Sand or Sand & Gravel</td><td colspan="4">Fine Sand, Silt, Loess, Loam</td><td colspan="4"></td></tr>
<tr><td>Unconsolidated Clay & Organic</td><td colspan="4"></td><td colspan="2">Peat</td><td colspan="3">Layered Clay</td><td colspan="4">Fat/Unweathered Clay</td></tr>
<tr><td>Consolidated Rocks</td><td colspan="4">Highly Fractured Rocks</td><td colspan="3">Oil Reservoir Rocks</td><td colspan="2">Sandstone</td><td colspan="2">Limestone, Dolomite</td><td colspan="2">Granite</td></tr>
</table>

Typical values for the hydraulic conductivity $K = K_x = K_y$ from the OptumCE materials manual.

Note that the ranges are very broad. It can't be expected to have accurate simulations without further study, through e.g. a pumping test or calibration with pressure measurements in early stages of a construction project. However, often approximate values are still useful. The hydraulic conductivity of Sands and Gravels suffice to be significantly larger than those of the materials like clay where excess pore pressures are build up. The dissipation of pore pressures is dominated by these layers of low hydraulic conductivity. The specific time scale of the dissipation may not be realistic, that is pressures may dissipate faster or slower than reality. But the process itself and distribution of pressures may still be useful.

3.3 Elasticity (Linear and Nonlinear)

Soil elasticity is far from trivial. Soil stiffness depends strongly on strain and stress. Therefore the stiffness is different at different depths in the same soil material. In this section, first linear elasticity is assumed and the various choices for linear elasticity are evaluated. It is observed that the choice for the elastic modulus depends on application. If the application is small strains like vibration due to traffic loads the stiffness is higher than for deformation near retaining walls. Next, a constant elasticity but depth dependent is described, and finally relations are given for nonlinear elasticity.

In more complex material models, elasticity is also included, because in the volume bounded by the yield surface behavior tends to be described elastically. Not all plasticity models allow sophisticated elastic behavior. Therefore it is necessary to be able to select suitable linear elastic parameter depending on application.

3.3.1 Linear elasticity

Linear elastic behavior may be isotropic or anisotropic. The most frequently used soil material models use isotropic elasticity, although some specialized models do employ anisotropy. Linear elasticity is specified by the Young's modulus E and the poisson's ratio ν. In soil material models sometimes the shear modulus G and bulk modulus K are used, these are related by:

$$G = \frac{E}{2(1+\nu)}, \qquad K = \frac{E}{3(1-2\nu)}$$

Figure 3.1 shows a typical soil triaxial test result of deviatoric stress $q = \sigma_1 - p_0$ versus axial strain ε_1. It is observed that there is no real definable elastic constant.

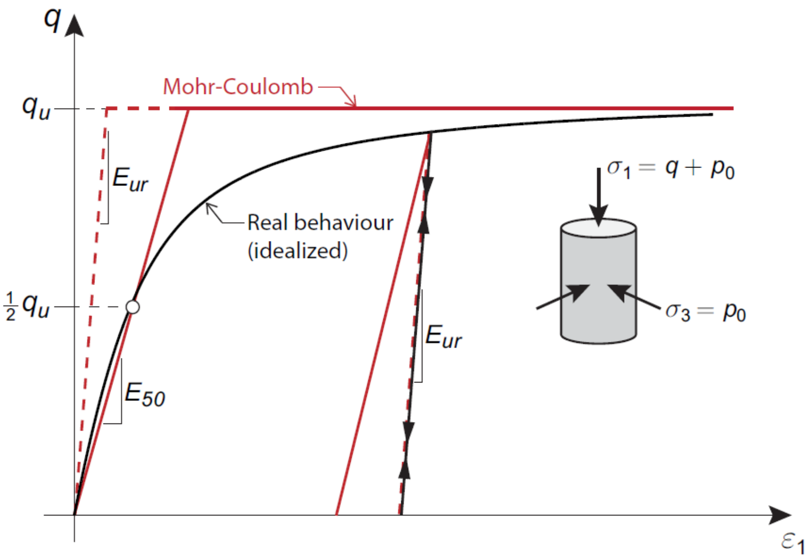

Figure 3.1. Real soil behavior and an approximation using the E50 Young's modulus and an unloading/reloading Young's modulus Eur (taken from the OptumCE manual).

Instead, the behavior is nonlinear with a gradually decreasing slope of the q, ε_1 curve until failure at stress q_u. It is common in geotechnics to use the E_{50} Young's modulus, which is defined as the slope of the line through the point on the q, ε_1 curve where half of the ultimate stress is reached: $q = 1\backslash 2 q_u$ and the origin of the graph. This is sometimes referred to as the secant stiffness for the point at $q = 1\backslash 2 q_u$. This is also the Young's modulus as prescribed by the Dutch code [NEN 9997-1+C2 table 2B].

Also depicted in Figure 3.1 is the stiffness during unloading/reloading behavior, E_{ur}. This stiffness is larger than the E_{50}. In some applications for example excavation, it is better to use this value. In more advanced models there is the possibility to include both, see section 3.5.

A general range of stiffness parameters for different soil types is given below. This range is rather large, partly because the effect of depth is already incorporated. Through analyses of Cone Penetration Test (CPT) data the actual values are more precisely determined at each depth.

parameter	**description**	**Range**[1,2,3]
E_{50}	Secant Stiffness at half ultimate deviatoric stress	15 – 110 MPa for clean sands 1 - 10 MPa for clays (lower values for soft clays, higher for solid) 0.5 - 2 MPa for organic clays 0.2 - 1 kPa for peats
E_{ur}	Unloading/ reloading stiffness	E_{ur} is 2-5 times E_{50}. Dutch code recommends 3 times E_{50}.

[1]*For more detailed ranges, see [NEN 9997-1+C2 table 2B]. Note that the upper range for stiffness found in [JCSS 2006] is larger, this is probably because these larger values are for small strains, not the E50, see also section 3.3.3.*

3.3.2 *Depth/confining stress dependence of the elastic stiffness*

A commonly used relation is

$$E_{50} = E_{50,ref} \left(\frac{-\sigma'_3 + c/\tan\phi}{p_{ref} + c/\tan\phi} \right)^m$$

Here σ'_3 is the minor principal effective stress (pressure is negative, hence $-\sigma'_3$ is positive in general). For normally consolidated soils σ'_3 is approximately the horizontal stress which can be computed from the vertical stress through the K_0 factor as discussed in section 2.3. c is the soil cohesion and ϕ the friction angle, see section 3.4. And $E_{50,ref}$ is the reference secant Young's modulus as defined in the previous section corresponding to the reference confining pressure p_{ref} (this can be interpreted as p_0 in a test like that of Figure 3.1). The power $m = 1$ for soft clays and a good approximation for sands is $m = 0.5$. Note that for sands the cohesion c is mostly negligible and the above equation reduces to a simple power law.

The above equation allows computation of Young's modulus E_{50} at different stress levels σ'_3 and hence at different depths. This equation cannot be used to describe the nonlinear stiffness behavior during a simulation because for a triaxial test the stress σ'_3 remains constant and hence the Young's modulus E_{50} is fixed. To describe the nonlinearity another model needs to used, see next section.

3.3.3 *Nonlinear elasticity*

Soils are in general nonlinear, as already shown in Figure 3.1. The hyperbolic model by [Duncan-Chang 1970] is a commonly used (e.g. in the Plaxis Hardening Soil model) to match the nonlinear behavior observed in triaxial tests. More recently it has been discovered that soil stiffness at very small strains is significantly higher than described by the hyperbolic model and more advanced models have been developed to accommodate this. A good summary of such small strain models is presented in [Benz 2007]. The main feature of nonlinear elasticity is that it leads to more localization of deformations. Deformations in the vicinity of say a retaining wall will be relatively larger due to the lower stiffness near the wall due to stress changes during installation, while soil further away at lower stress changes responds stiffer. This leads to behaviour better in agreement with observations, see [Benz 2007]. Both the hyperbolic and small strain elastic models are discussed because some FEM packages are able to model the former but not the latter. Both models lead to an improvement in soil behavior. But the small strain model is superior in that it can be extended to include soil-hysteresis effects and as such be used for cyclic loading.

3.3.3.1 *Hyperbolic Duncan-Chang model*

A commonly used nonlinear elastic description for soils is the [Duncan-Chang 1970] hyperbolic model:

$$-\varepsilon_1 = \frac{1}{E_i}\frac{q}{1 - q/q_a}$$

With q the deviatoric stress defined earlier, q_a the asymptotic ultimate deviatoric stress and E_i the initial stiffness. It is clear that if q_a is taken to be the failure stress problems will arise because an attempt is made to model plasticity with elasticity. It is therefore better to take q_a somewhat higher than the failure stress. This is shown in Figure 3.2.

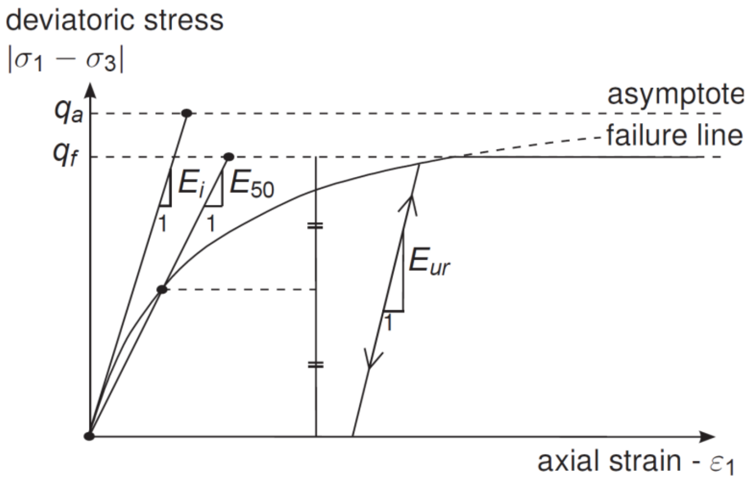

Figure 3.2. Hyperbolic model use and description.

In Plaxis, the ratio $R_f = q_f/q_a$ is used, where q_f is the failure stress, and a value of 0.9 is used by default. This is a way to have plasticity describe actual failure and elasticity the nonlinear part up to failure. It leads to a discontinuity in the slope of the curve but this is also the case for a linear elastic perfect plastic model. The hyperbolic model is a considerable improvement for soil behavior.

In section 3.3.1, the E_{50} Young's modulus was derived and ranges were given. Based on the E_{50} how can the initial stiffness E_i be determined? This is achieved by computing the strain at half the failure stress, that is $q = \frac{1}{2}q_f = \frac{1}{2}R_f q_a$. If this is substituted in the hyperbolic equation it is found:

$$-\varepsilon_{1,50} = \frac{1}{E_i}\frac{\frac{1}{2}R_f q_a}{1-\frac{1}{2}R_f q_a/q_a}$$

And E_{50} is the secant stiffness in this point, hence:

$$E_{50} = \frac{\frac{1}{2}R_f q_a}{-\varepsilon_{1,50}} = E_i\left(1-\frac{\frac{1}{2}R_f q_a}{q_a}\right) = E_i\frac{2-R_f}{2}$$

And using the E_{50} the initial stiffness is computed to be:

$$E_i = \frac{2E_{50}}{2-R_f}$$

It is clear that the hyperbolic model is best used in combination with a plasticity model to prevent problems close to failure. Below the failure line the hyperbolic nonlinear elastic model can be used, but the parameter q_a or similar must be specified and, to do this properly, information about failure needs to be known.

3.3.3.2 Small strain nonlinear elastic model

Experiments show that when plotting shear strain on a logarithmic scale, the secant shear modulus vs shear strain is an S-curve, see Figure 3.3. The ranges of strains in some geotechnical applications are shown, as well as the range from conventional soil testing, e.g. triaxial tests. From this, it is observed that the soil stiffness found using triaxial tests can be significantly lower than the stiffness in the limit where strains go to zero. This is commonly referred to as G_0.

In literature, several relations can be found for this S-curve. A well-known relation is that of [Hardin-Drnevich 1972], which was modified by [Santos & Correia 2001] to be applicable more generally. An often used relation especially for earthquake engineering is the curve by [Darendeli 2001]. Here we single out [Santos & Correia 2001] because it is used in the Plaxis Hardening soil small strain model. It should be straightforward to convert the analysis here to similar models in other FEM packages.

Figure 3.4 shows the S-curve by [Santos & Correia] with experimental data. This curve is normalized to the small strain shear modulus G_0 and to the shear strain $\gamma_{0.7}$ where the secant shear modulus is 0.7 times G_0. The S-curve shape is fixed and with these two normalization parameters a wide variety of soil types match this S-curve. Therefore knowing G_0 and $\gamma_{0.7}$ is sufficient to fix the behavior. This small strain shear modulus G_0 can be determined from seismic cone penetration tests or, but with some more uncertainty, from more common Cone Penetration Test data using software shown in Chapter 4. For problems of wave propagation related to (train) traffic, the strains are very small and using a linear elastic model based on the small strain shear modulus G_0 is recommended over e.g. the E_{50}.

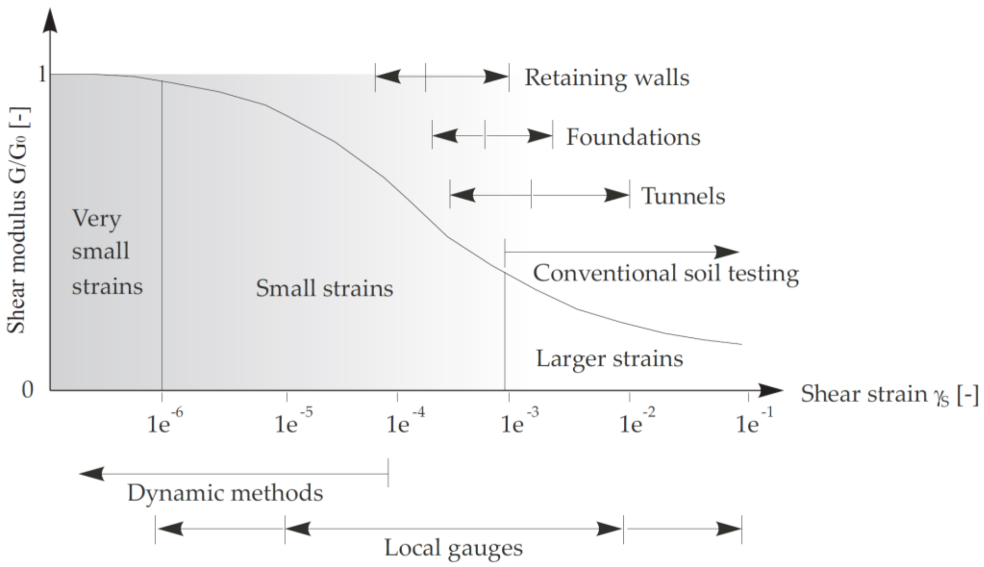

Figure 3.3. Ratio of secant shear modulus to small strain shear modulus G_0 as a function of shear strain with application ranges (from the Plaxis manual, after [Attkinson & Sallfors 1991])

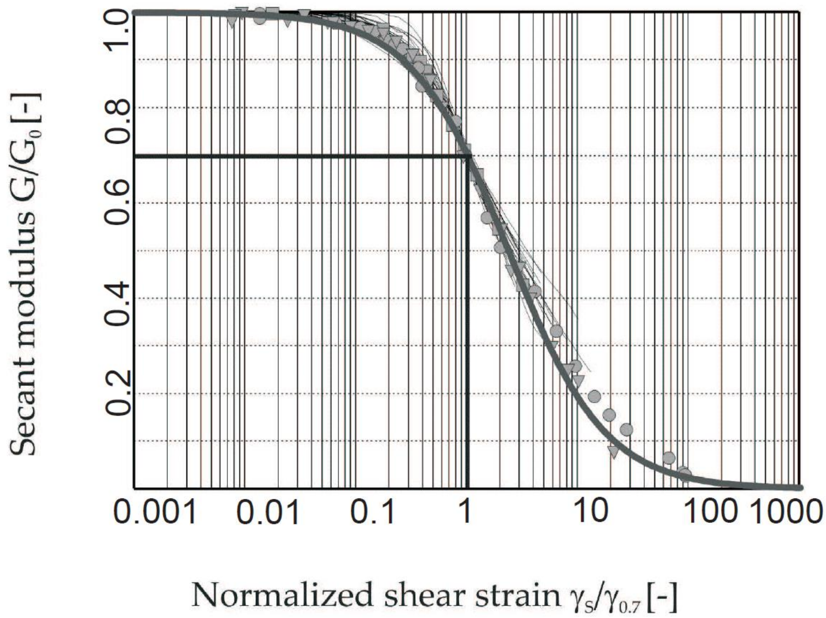

Figure 3.4. Hardin-Drnevich "s-curve" compared to test data, after [Santos & Correia 2001], plot from the Plaxis manual.

The [Santos & Correia 2001] S-curve is given by:

$$\frac{G}{G_0} = \frac{1}{1 + a\left|\frac{\gamma}{\gamma_{0.7}}\right|}, \qquad a = 0.385$$

Here G is the secant shear modulus and γ the shear strain. In the Plaxis manual it is remarked that if $\gamma = \gamma_{0.7}$ that $\frac{G}{G_0} = 0.722$ and that the 0.7 is in fact rounded off. Because of the secant modulus, the shear stress τ can be computed as $\tau = G\gamma$, which means that the shear stress is:

$$\tau = G_0 \frac{\gamma}{1 + a\left|\frac{\gamma}{\gamma_{0.7}}\right|}$$

Note that the S-curve is defined in terms of shear modulus and shear strain, while the hyperbolic modulus in the previous section is defined in terms of the Young's modulus and axial strain. In Annex A there are some concepts worked out to express one in the other. The reason for using the small strain model is shown in Figure 3.5 which shows settlement measurements and simulations during tunnel construction. Shown are simulations with the small-strain model and hardening soil model (HS) which uses the hyperbolic elasticity model. The small strain model matches better observation due to the fact that it leads to more localization of the deformations. In soil, the region further away from a construction site has very small strains and behaves more stiff, while nearer to a construction site the strains are larger and the behavior is softer. Linear elasticity does not account for this fact, hyperbolic elasticity to some extent, and the small strain elastic model to a more realistic extent.

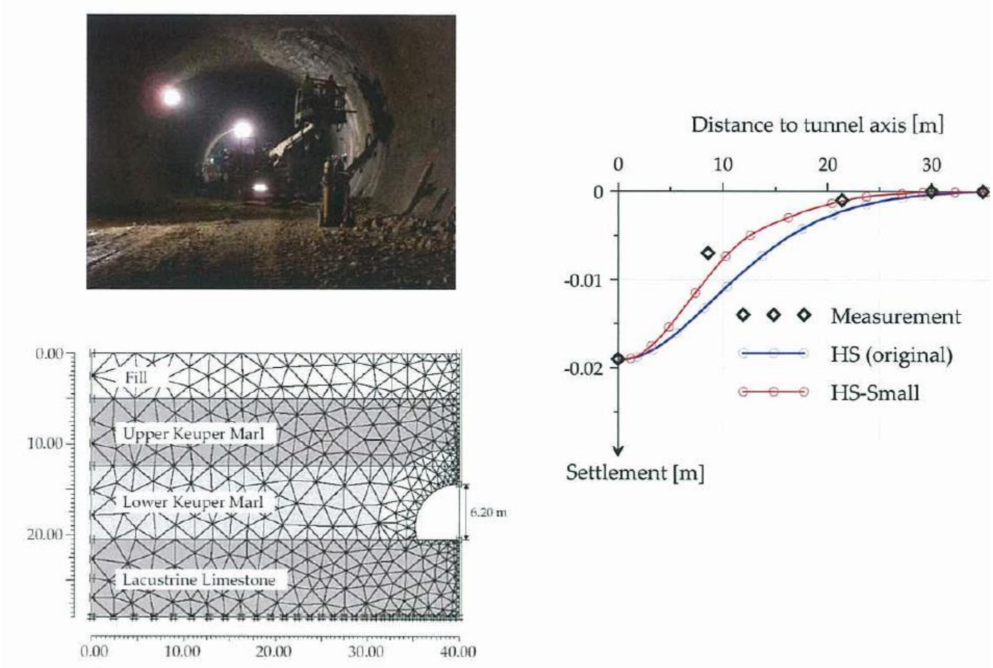

Figure 3.5 settlement during construction of Steinhaldenfeld NATM tunnel from Benz (2007).

3.3.4 *Unloading/Reloading*

From Figures 3.1 and 3.2 it can be seen that the unloading/reloading stiffness is in general much larger than the E_{50} stiffness or the tangent stiffness in the nonlinear stress strain curve. Ranges for E_{ur} have been given in the table in section 3.3.1.

Normally the unloading/reloading behavior can only be modelled using an elasto-plastic model with partial memory specified by the pre-consolidation pressure (see section 3.5). But in some cases where it is known that the simulated case is that of unloading/reloading, this larger stiffness E_{ur} could be used. These cases are not common however and it is recommended to use unloading/reloading with a proper elasto-plastic model to prevent simulation errors.

3.4 Plasticity models without memory

Soil plasticity describes soil (shear) failure. It is dependent on stress state but not on stress history. It is generally accepted that a suitable yield surface for soils is the Mohr-Coulomb yield surface shown in Figure 3.6.

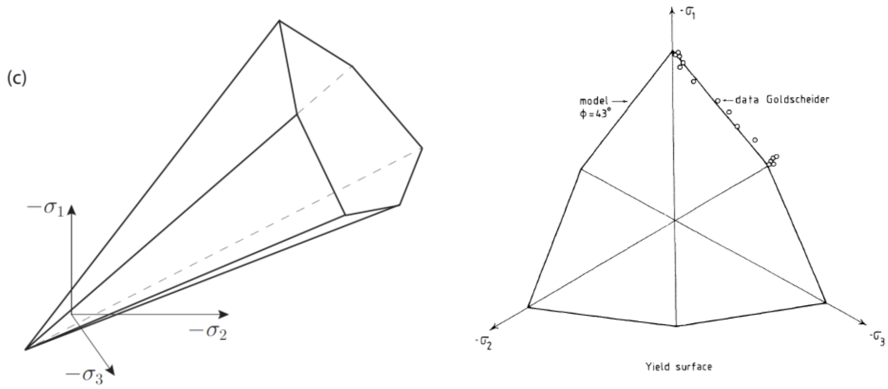

Figure 3.6. Mohr-Coulomb yield surface. In three dimensional principal stress space (left) and in the deviatoric plane with experimental data on dense sand (right).

Inside the yield surface, the behavior is elastic and can be modelled as described in the previous section. The Mohr-Coulomb yield surface is described by two parameters, the cohesion c and the friction angle φ. The friction angle determines slope of the cone while the cohesion is the offset. If cohesion is zero, the cone starts in the stress origin. If nonzero, tension is allowed. The original Mohr-Coulomb model is not good enough for soil modelling in many applications, because the volumetric strain during plastic flow is too large. To solve this, in most FEM packages the dilatancy angle is introduced and the plastic flow potential of the Mohr-Coulomb model is governed by this dilatancy angle rather than the friction angle. This is called non-associated plasticity.

Figure 3.7 demonstrates the concept of dilatancy. In this case the elastic behavior is linear. In the top graph the deviatoric stress increases linearly with axial strain ε_1 up to the point of failure after which the shear stress remains constant. In the bottom curve it is visible that there is contraction (negative volumetric strain) under elastic compression due to a poisson's ratio <0.5. Then from the point of failure there is positive volumetric strain depending on the dilatancy angle ψ. In the original Mohr-Coulomb model this angle is $\psi = \varphi$ by default. This is called associative plasticity. It turns out that the volumetric strain for associated is too large. [Vermeer & de Borst] show that only $\psi < \varphi$ is correct from thermodynamic considerations. In practice ψ is significantly smaller, see the table below.

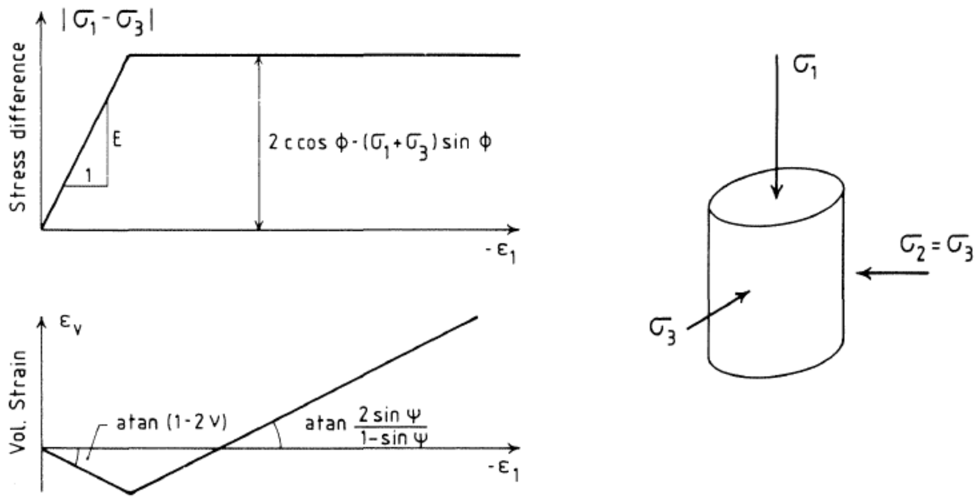

Figure 3.7. The concept of dilatancy through simulation results of a triaxial test using a linear elastic perfectly plastic Mohr-Coulomb model with dilatancy [Vermeer & de Borst 1984]

In general non-associative Mohr-Coulomb plasticity is superior and more realistic compared to associative Mohr-Coulomb plasticity. For bearing capacity simulations, in terms of limit loads, the differences are small. But in terms of deformation and other types of analyses the differences may be significant, see [Vermeer & de Borst 1984].

A general range of associative Mohr-Coulomb parameters for different soil types is given below:

parameter	**description**	**Range[1,2,3]**
c	Cohesion [kPa]	0 kPa for clean sands 0 - 30 kPa for clays (lower for soft clays, higher for solid) 0 - 10 kPa for organic clays 2 - 10 kPa for peats
φ	Friction angle [deg]	30 – 40 degrees for sands (high values for more dense) 15 - 30 degrees for clays (lower for soft clays, higher for more sandy clays) 13-16 degrees for organic clays 13-16 degrees for peats
ψ	Dilatancy angle [deg]	In general $\psi < \varphi$ and is in the range of 0 to 20 degrees [Vermeer & de Borst 1984] $\psi = 0$ degrees for clays $\psi = \varphi - 30$ if $\varphi > 30$ and $\psi = 0$ otherwise for sands [Brinkgreve 2010]

[1]For more detailed ranges, see [NEN 9997-1+C2 table 2B] or [JCSS 2006].
[2]For dilatancy, neither NEN6740 nor JCSS have guidelines. Therefore estimators from other literature are provided. Dilatancy cut-off and tension-cut off are optional parameters that may be unavailable in some FEM packages.
[3]For plane-strain simulations, for sand type materials, the friction angle is about 1.1 times the friction angle in the table, see [Kulhawy & Mayne 1990] figure 4-11.

3.4.1 Some comments on the use of plasticity models

Based on modelling and simulation experience, some comments are made that may be relevant for the application of non-associated Mohr-Coulomb plasticity:

- Although soil non-associative behavior with $\psi \neq \varphi$ is more realistic, it is more difficult numerically and can lead to numerical instabilities and bifurcations [Vermeer & de Borst 1984] that may make it difficult to complete a simulation. In some FEM packages it may be necessary to force $\psi = \varphi$ and use associative behavior instead

- Some FEM packages have numerical difficulty with a cohesion of zero (common for sands) in these cases it is beneficial to set cohesion to a small value, e.g. 1 kPa. This will hardly affect the material behavior.
- Some FEM packages have numerical difficulty with setting friction angle to zero (which sometimes is preferred when modeling equivalent undrained behavior). In that case it may be beneficial to set the friction angle to a small value, e.g. 1 degree. This will hardly affect the material behavior.
- The 6 planes of the Mohr-Coulomb yield surface enable different failure stresses for triaxial extension and compression. This is realistic soil behavior as demonstrated in Figure 3.6. Yield surfaces with circular cross section are not able to do this, such as the Von Mises and Drucker Prager yield surfaces and are therefore not preferred for geotechnical application. Also, the Mohr-Coulomb yield surface is cone shaped, meaning more shear resistance at higher stress. Yield surfaces that do not depend on isotropic stress, such as the Tresca yield surface are less suitable, unless in calculations that are effectively undrained. It is recommended to, in order to correctly model soil behavior, select material models in FEM packages with a yield surface that approximate the Mohr-Coulomb yield surface as closely as possible. There exist models such as the Matsuoka-Nakai yield surface that are approximations of Mohr-Coulomb but without the discontinuities at the edges where planes connect. These are also suitable. In Abaqus, the more advanced materials for soil can only be described by a Modified Drucker Prager model. This model has a K parameter to deform the circular cone Drucker Prager yield surface to be more akin to Mohr-Coulomb.
- For plane strain simulations it is possible to use Drucker Prager instead of Mohr-Coulomb by making the inner fit as shown in figure 3.8 below. This is because triaxial compression does not exist as such in a plane strain setting. The OptumCE materials manual has a table converting Mohr-Coulomb parameters to Drucker Prager in this case.

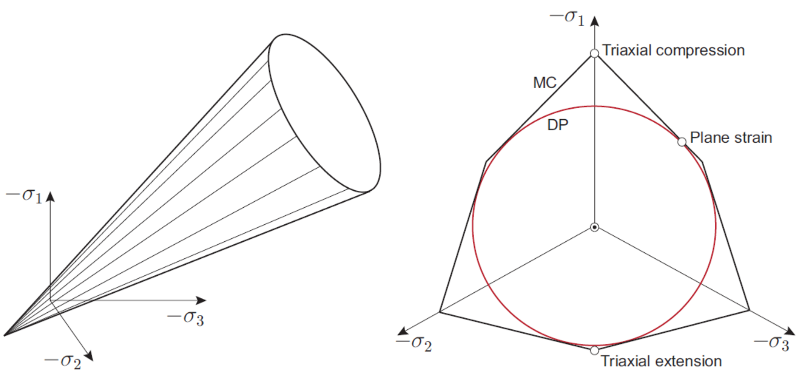

Figure 3.8 Drucker-Prager (DP) cone and matching to Mohr-Coulomb (MC) criterion in plane strain (From Optum CE materials manual)

3.4.2 *Advanced options for Mohr-Coulomb plasticity*

Two advanced options available in some FEM packages for Mohr-Coulomb plasticity are discussed here. These are dilatancy cut-off and tension cut-off. Dilatancy cut-off is used to simulate more realistic behavior for sands and tension cut-off is used to simulate more realistic behavior for clays.

3.4.2.1 *Dilatancy cut-off*

Geomaterials can't have an infinite increase in volumetric strain, which is what the Mohr-Coulomb model with a positive dilatancy angle predicts. When the soil grains become very loosely packed during dilatancy to the point of maximum void ratio, the volumetric strain cannot increase anymore and the dilatancy angle from then on is effectively zero. This is demonstrated in Figure 3.9 Material models which incorporate such dilatancy cutoff yield more realistic behavior for larger plastic strains.

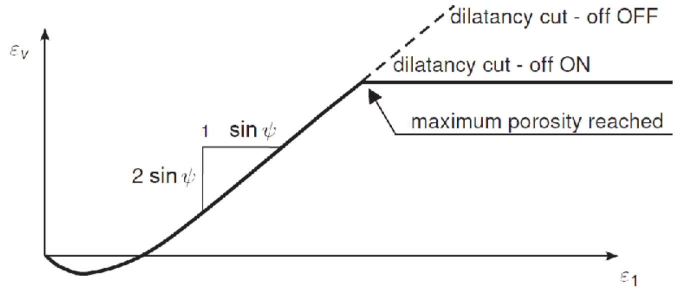

Figure 3.9 dilatancy cut off (from the Plaxis material models manual)

To model a dilatancy cutoff the material model needs to have information about the maximum porosity, that is the porosity where a soil type reaches the point of zero volumetric strain. For example, in Plaxis, the user needs to specify an initial porosity and a maximum porosity. Turning on dilatancy cutoff then gives the expected behaviour. In OptumCE this dilatancy cutoff is specified in terms of a critical volumetric strain $\varepsilon_{v,cr}$ as the measure after which dilatancy is cutoff. Diana does not have a dilatancy cutoff as such, but the Modified Mohr-Coulomb model does lean on the critical state soil mechanics theory where the point of maximum porosity is also given by the point where the soil friction angle is the critical state angle. Then in Diana a friction hardening can be specified effectively modelling a dilatancy cutoff. The table below summarizes the options and in which case to use dilatancy cut-off:

parameter	**description**	**Range**
On/off	Dilatancy cutoff	Off: ψ is constant and equal to user input (use for clay) On: ψ is equal to the user input for void ratio $<e_{max}$ and $\psi = 0$ for void ratio= e_{max} (use for sands)

use of dilatancy cut-off

3.4.2.2 *Tension cut-off*

Besides dilatancy cutoff, some FEM packages (Plaxis, OptumCE) have a tension cutoff option for the models using the Mohr-Coulomb yield surface. Tension is possible in Mohr-Coulomb when the cohesion c is non-zero. However the soft clays hardly can handle tension, even though the cohesion is nonzero. By default in Plaxis tension cutoff allows zero tension when turned on. But the value of allowed tension can be manually set. The most common use case for tension cut off is for undrained modelling for clay. In this case an undrained shear strength is modelled with the cohesion in the Mohr-Coulomb model, this allows a corresponding tensile stress which may be unwanted. Setting a tension cut-off allows for input of the correct values for both shear strength and tensile strength

parameter	description	Range
On/off	Tension cutoff	Off: maximum tension is related to the cohesion in the Mohr-Coulomb cone, always use for sands. On: maximum tension is user specified. Use for clays to reduce tensile strength where the cohesion is such that a situation can occur where tensile strength is exceeded

Use of tension cut-off

3.5 Elasto-plasticity models with pre-consolidation pressure (partial memory)

The plasticity model described in section 3.4 depends only on stress state, not on stress history. It is observed in particular in soft soils that the stress-strain relation has a bend at a certain stress level after which the behavior becomes softer (in log space), see Figure 3.10. This stress level is called the pre-consolidation pressure. The concept behind this is that the soil has been loaded to a larger pressure in the past and subsequently unloaded. This can be either geological due to e.g. loading of soil with a thick ice sheet during the ice age, or due to unloading during excavation, or pre-loading and unloading of embankments for road/railway construction. Reloading shows then a stiff behavior and going past the pre-consolidation pressure point yields a softer behavior. This is observed for soft soil samples taken from depth and tested in the laboratory loaded from zero pressure up to the pressure at depth and beyond. If the pre-consolidation pressure (the bend in the loading graph) is at a pressure corresponding to the soil weight at the depth from which the sample was taken, the soil is normally consolidated. If it is at a higher pressure the soil is over-consolidated.

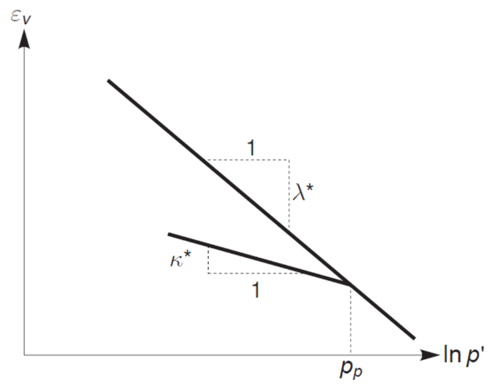

Figure 3.10. Logarithmic relation between volumetric strain and mean stress as typical for soft soils, the stiffer unloading-reloading branch up to the pre-consolidation pressure p_p is indicated as well (Taken From the Plaxis manual).

The degree of overconsolidation is often described with the Over Consolidation Ratio (OCR). The OCR is defined as the ratio of the maximum pre-consolidation vertical effective stress to in situ vertical effective stress:

$$OCR = \frac{\sigma'_{v,p}}{\sigma'_{v,0}}$$

An $OCR = 1$ is normally consolidated soil and $OCR > 1$ is overconsolidated soil. The OCR is a parameter that can be estimated from CPT data as shown in Chapter 4. In some FEM packages, the OCR can be specified as a material parameter, or per layer from which a material model internally computes the pre-consolidation pressure p_p as a state parameter for each integration point. If loading takes place beyond the pre-consolidation pressure, this state parameter is updated such that it is always possible to discern loading-reloading for pressures below p_p and virgin loading for pressures above p_p (actually pressures are never above p_p because it is updated during virgin loading).

Besides the OCR to model the behavior shown in Figure 3.10 a material model must be able to describe unloading/reloading behavior related to the preconsolidation pressure. Examples are the (small strain) Hardening soil model or soft soil model in Plaxis, the Hardening Mohr Coulomb model or Modified Cam Clay models in OptumCE, the cap hardening model in Abaqus, or the Modified Mohr Coulomb model in DIANA. Besides these it must be noted that the in-situ horizontal stress differs for an overconsolidated soil compared to a normally consolidated soil, which means that a different value of K_0 must be specified to compute initial stresses as mentioned in section 2.3, equations (2.1) and (2.2).

The way these types of material models are implemented is shown in Figure 3.11. A “cap” is defined in stress space from the preconsolidation pressure to the shear failure line. The area within these boundaries is elastic and operates using unloading and reloading stiffness E_{ur} or the κ^* for soft soils as in Figure 3.10. When the soil pressure reaches the preconsolidation pressure and further increases, this cap is shifted. During the shift takes place what is called as “cap-plasticity” which is a softer behavior as specified in these material models by the λ^* in Figure 3.10, or elastic behavior depending on the chosen material model.

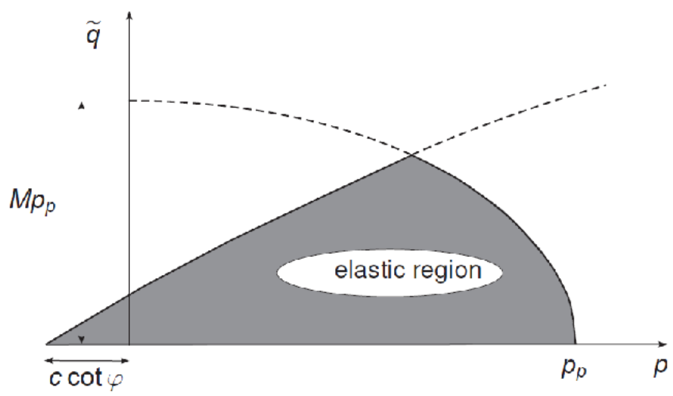

Figure 3.11. Yield surfaces of the Hardening Soil model in Plaxis. The preconsolidation pressure p_p indicates the position of the so called “cap” which

shifts with the p_p *to enlarge the elastic region. Unloading-reloading takes place in the elastic region until the cap is reached or the failure line.*

4 Soil classification and parameter estimation from Cone Penetration Tests (CPT)

The most readily available type of soil data are Cone Penetration Tests (CPT). For the Netherlands in particular, the service www.dinoloket.nl contains a database of many CPT's which can be requested for download by selecting an area and checking what CPT's have been performed there. Much work has been carried out to estimate soil layer type and parameters from CPT data. Most of the developments have been consolidated in [Robertson 2009] and [Robertson & Cabal 2015]. A CPT contains the cone resistance and sleeve friction as a function of depth. Sometimes the water pressures are measured as well, or they can be estimated from the phreatic level. These 3 quantities as a function of depth allow soil classification and parameter estimation. The equations in [Robertson 2009] and [Robertson & Cabal 2015] can readily be implemented in e.g. Excel for this goal. But currently this has not been done. Instead the software CPT-iT3 from GeoLogismiki is used here to show the easy with which parameters can be determined. The output of the software does not cover all parameters needed for the material models described in the previous chapter. It is shown how additional parameters can be derived from the output of the software to complete the list.

4.1 Example CPT's from Dinoloket.nl

To demonstrate parameter estimation, 5 CPT's are selected at the location of the TNO Structural dynamics lab, using the public www.dinoloket.nl website. After selecting the CPT's, see Figure 4.1, the CPT data is send by email.

Figure 4.1. Dinoloket map and selected CPT's.

4.2 Soil classification from CPT data

The raw CPT data from one of the five points is shown in Figure 4.2, and the CPT-iT3 software soil behavior type classification according to [Robertson 2009] is shown in Figure 4.3. The resulting soil profile with layers in Figure 4.4.

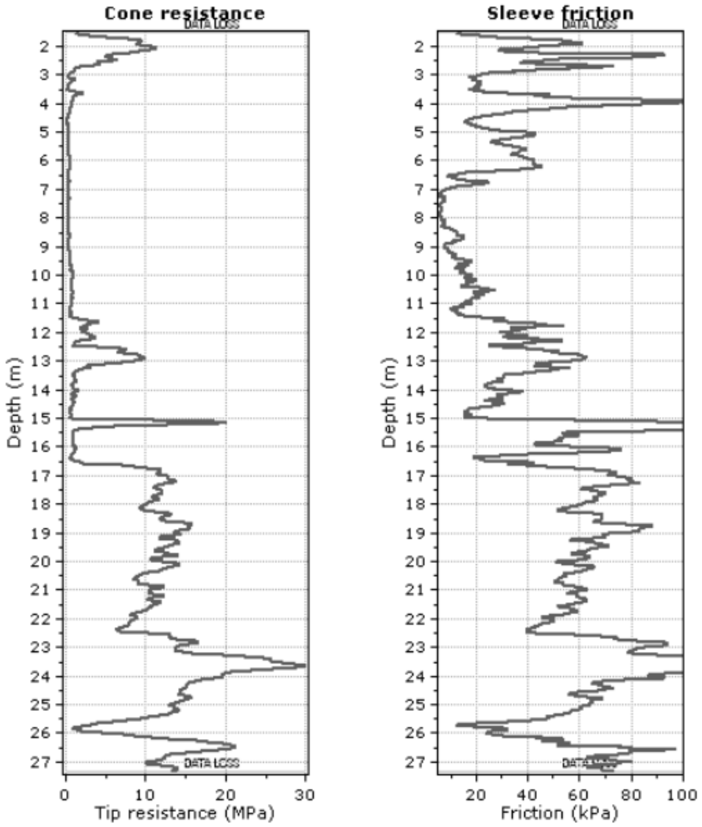

Figure 4.2. Raw CPT data, cone resistance and sleeve friction

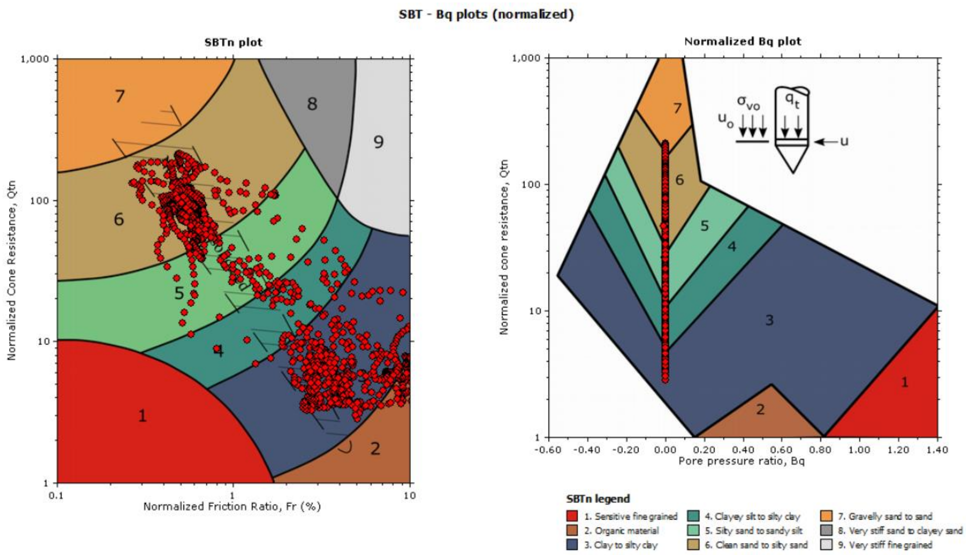

Figure 4.3. CPT-iT3 soil classification, [Robertson 2009] soil behavior types from the CPT in figure 4.2

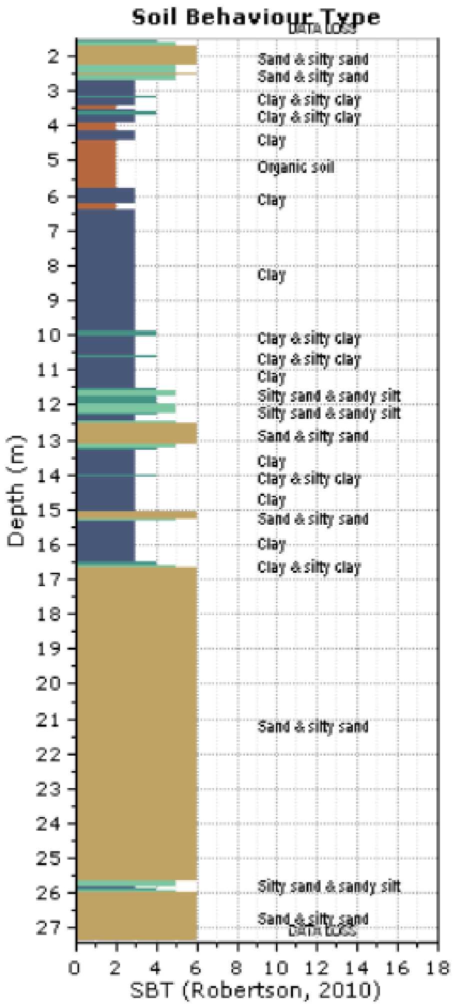

Figure 4.4 Soil layers classified in terms of [Robertson 2009] soil behavior type.

4.3 Estimated parameters

The CPT-iT3 software estimates soil parameters using equations from [Robertson 2009] and can Export an excel sheet with estimated parameters. This sheet contains:

1. Soil density
2. Total and effective vertical stress
3. Permeability
4. Young's modulus (for SBT….)
5. Small strain Shear modulus (for all materials)
6. Friction angle (for sand type materials)
7. Shear strength (for clay type materials)
8. Shear wave velocity
9. Over consolidation ratio (OCR)
10. Relative density

These should be sufficient to generate input for the models discussed in chapter 3.

A few notes:

- From the shear wave velocity v_s, the small strain shear modulus can be computed using $G_0 = \rho v_s^2$, where ρ is the density which is also estimated from the CPT.
- In the estimation software a friction angle is estimated for sand like materials, while an undrained shear strength is estimated for clay like materials. The treatment of undrained behavior for clays is not discussed in full here. One approach is to use the density and OCR to determine the stresses at the depth where the soil is present and to compute a friction angle cohesion using ratio's from the table in Chapter 3 that match the undrained shear strength. The topic of undrained behavior is complex.

5 Conclusions and recommendations

This document gives an overview of geotechnical modelling from the perspective of engineers well versed in FEM, but less familiar with geotechnical modelling and parameter estimation. The importance of a correct initial stress state is discussed and methods to model the initial stresses, in particular the lateral stresses are given. Following these guidelines can prevent some of the most common modelling mistakes. The most commonly used material models are discussed with parameter ranges for common soil materials that serve as a sanity check when confronted with soil layer parameter determination. Soil classification and parameter estimation through CPT data is discussed, using the CPeT-IT3 software which is bought during this project and is a practical tool to determine input parameters for FEM simulations. These best estimate parameters can be used as medians for probabilistic soil description. This is not discussed in detail here, but the [JCSS 2006] gives distributions for the most relevant soil parameters in this document and other parameters, such as soil dilatancy, treated here are correlated to the parameters for which distributions exist. The relations provided here are sufficient to build up a probabilistic soil model.

5.1 Recommendations

To make the information in this report easier to use in practice the following recommendations are made:

- Implement the relatively simple equations for CPT soil classification and parameter estimation in a form that is more suitable for general use in TNO, such as excel or Python.
- Work with the Geomodelling group of TNO Utrecht to use the probabilistic geological model of the top 60 m surface of the Netherlands (GeoTop) in simulations. To do so, the GeoTop model needs to be extended to incorporate probabilistic distributions of soil material parameters as discussed here. For Groningen this has been carried out to be able to run probabilistic analyses of nonlinear site response
- Using the approach in this document, best estimate soil parameters vary over a soil layer. It needs to be investigated if the uncertainty of soil parameters in [JCSS 2006] incorporates this variation, or that this variation within a layer based on CPT interpretation must be explicitly taken into account.
- It needs to be determined if the Young’s modulus estimated from the CPT equations by [Robertson 2009] is the E50 or that it corresponds to another definition. In the current document the E50 is used to define the elastic behavior.
- It needs to be determined what the expectation value is for the N factor in the [Robertson 2009] equations to compute the undrained shear strength from the cone resistance. The N factor that is used by default in CPeT-IT3 probably is based on a characteristic value.
- Modelling undrained behavior for soft soils is not treated in detail in this document. Soft soils are common, however, and it is recommended to write additional guidelines regarding undrained behavior, in particular the mapping of undrained shear strength to friction and cohesion parameters.

- A detailed overview of what material models in which FEM packages should be used is not presented here. An inventarisation of FEM packages used in TNO for geomodelling is recommended as well as a making a thorough set of test simulations, benchmarking the different material options, with the intent to derive a mapping between the material models leading to consistent results in modelling. An obvious example would be the Plaxis Hardening soil model and comparable models in DIANA (Modified Mohr Coulomb), OptumCE (Hardening Mohr Coulomb) and Abaqus (Cap Hardening model). Both modelled triaxial tests, shear tests with loading and unloading are recommended for different initial conditions to evaluate stress dependent stiffness and shear failure and preconsolidation behavior.
- Different geotechnical modelling methods outside of the FEM are not treated here. It is recommended to provide an overview of the most useful of these methods with a mapping of the work here to the input parameters required for these models. Obvious examples are methods to compute springs and dashpots for soil structure interaction or dynamic soil structure interaction for sheet pile walls, slab and piled foundations, monopiles (offshore) and strip foundations. Several methods exists with different methods being suitable for different applications.

6 References

[Atkinson & Sallfors 1991] J.H. Atkinson, G. Sallfors, experimental determination of soil properties, proc. 10th ECSFME 3, 915-956

[Benz 2007] T. Benz, Small strain stiffness of soils and its numerical consequences, PhD thesis Stuttgart university, 2007

[Brinkgreve 2010] Validation of empirical formulas to derive model parameters for sands, R.B.J. Brinkgreve, E. Engin, NUMGE 2010

[Darendeli 2001] Darendeli, M.B. Development of a new family of normalized modulus reduction and material damping curves. Ph.D. dissertation, University of Texas, Austin, 2001

[Duncan & Chang 1970] Nonlinear analysis of stress and strain in soils. Journal of the Soil Mechanics and Foundation division (ASCE), vol 96, SM5, 1970

[Hardin & Drnevich 1972] Hardin, B.O., and Drnevich, V.P. Shear modulus and damping in soils: measurement and parameter effects. Journal of Soil Mechanics & Foundations Division, 1972, 98(6): 603–624.

[Kulhawy & Mayne 1990] F.H. Kulhawy, P.W. Mayne, Manual on estimating soil properties for foundation design, Electric Power Research Institute (EPRI), 1990

[JCSS 2006] Probabilistic Model Code, Section 3.7: SOIL PROPERTIES, Updated version August 2006, by J. Baker and E. Calle (Original version: July 2002 by R.Rackwitz / H.Denver / E.Calle)

[NEN 9997-1+C2] Geotechnical design of structures - Part 1: General rules

[Mayne & Kulhawy 1982] P.W. Mayne, F.H. Kulhawy, OCR – K0 relationships in soils, Journal of the Geotechnical Engineering Division · June 1982

[Robertson 2009] P.K. Robertson, Interpretation of cone penetration tests, a unified approach, Canadian Geotechnical Journal, 46: 1-19

[Robertson & Cabal 2010] P.K. Robertson and K.L. Cabal, Estimating soil unit weight from CPT, 2nd International Symposium on Cone Penetration Testing, Huntington Beach, CA, USA, May 2010

[Robertson & Cabal 2015] P.K. Robertson and K.L. Cabal, Guide to Cone Penetration testing, 6th edition, 2015

[Santos & Correia 2001] J.A. Santos, A.G. Correia, Reference threshold shear strain of soil. It's application to obtain a unique strain-dependent shear modulus curve for soil. Proceedings 15th International Conference on Soil mechanics and Geotechnical Engineering. Istanbul, Turkey, volume 1, 267-270

[Vermeer & de Borst 1984] Non Associated plasticity for soils and rock, P.A. Vermeer, R. de Borst, Heron vol 29, 1984, no 3.

[Verruijt 2012] Soil Mechanics, A. Verruijt, 2012

7 Annex A Small strain model and hyperbolic model

The [Santos & Correia 2001] S-curve for the small strain model is given by:

$$\frac{G}{G_0} = \frac{1}{1 + a\left|\frac{\gamma}{\gamma_{0.7}}\right|}, \qquad a = 0.385$$

Here G is the secant shear modulus and γ the shear strain. In the Plaxis manual it is remarked that if $\gamma = \gamma_{0.7}$ that $\frac{G}{G_0} = 0.722$ and that the 0.7 is in fact rounded off.
Because of the secant modulus, the shear stress τ can be computed as $\tau = G\gamma$, which means that the shear stress is:

$$\tau = G_0 \frac{\gamma}{1 + a\left|\frac{\gamma}{\gamma_{0.7}}\right|}$$

Using the mean and deviatoric stress invariants

$$p = \frac{\sigma_{ii}}{3}$$

$$q = \sqrt{\frac{3}{2}\left(\sigma_{ij} - \frac{1}{3}\delta_{ij}\sigma_{kk}\right)\left(\sigma_{ij} - \frac{1}{3}\delta_{ij}\sigma_{kk}\right)}$$

And volumetric and equivalent strain invariants

$$\varepsilon_v = \varepsilon_{ii}$$

$$\varepsilon_q = \sqrt{\frac{2}{3}\left(\varepsilon_{ij} - \frac{1}{3}\delta_{ij}\varepsilon_{kk}\right)\left(\varepsilon_{ij} - \frac{1}{3}\delta_{ij}\varepsilon_{kk}\right)}$$

Where the σ_{ij} and ε_{ij} are the stress and strain components and the Einstein summation index is used. Using these relations and applying them to a shear test where $\sigma_{12} = \sigma_{21} = \tau$, $\varepsilon_{12} = \varepsilon_{21} = \gamma/2$ and all other components zero, it is found that

$$\tau = q/\sqrt{3}$$
$$\gamma = \varepsilon_q\sqrt{3}$$

Applying the relations to a triaxial test where $\sigma_{11} = \sigma_{axial}, \sigma_{22} = \sigma_{33} = \sigma_{lateral}$ and $\varepsilon_{11} = \varepsilon_{axial}, \varepsilon_{22} = \varepsilon_{33} = \varepsilon_{lateral}$ and all other components zero, it is found that:

$$q = \sigma_{axial} - \sigma_{lateral}$$

$$\varepsilon_q = \frac{2}{3}(\varepsilon_{axial} - \varepsilon_{lateral})$$

The correctness of these relations can be tested for linear elasticity where it is known that $\tau = G\gamma$, $q = E\varepsilon_{axial}$ and through the poisson's ratio $\varepsilon_{lateral} = -\nu\varepsilon_{axial}$. Then from the top relation

$$\frac{q}{\sqrt{3}} = G\varepsilon_q\sqrt{3} \rightarrow q = 3G\varepsilon_q$$

And from the bottom relation

$$\varepsilon_q = \frac{2}{3}|\varepsilon_{axial} - \varepsilon_{lateral}| = \frac{2}{3}(1+\nu)|\varepsilon_{axial}|$$

And therefore

$$q = E\varepsilon_{axial} = \frac{3E}{2(1+\nu)}\varepsilon_q$$

Then it should hold that

$$G = \frac{E}{2(1+\nu)}$$

Which is indeed the case. Using the invariants now shear test results can be written in terms of q and $\varepsilon_{axial}, \varepsilon_{lateral}$:

$$\tau = q/\sqrt{3}$$

$$\gamma = \varepsilon_q\sqrt{3} = \frac{2}{\sqrt{3}}(\varepsilon_{axial} - \varepsilon_{lateral})$$

Substituting these in the [Santos & Correia 2001]:

$$q = G_0 \frac{2|\varepsilon_{axial} - \varepsilon_{lateral}|}{1 + a\left|\frac{\frac{2}{\sqrt{3}}(\varepsilon_{axial} - \varepsilon_{lateral})}{\gamma_{0.7}}\right|}$$

Using negative axial strains (compression) and assume a constant poisson's ratio ν, it follows that

$$q = E_0\frac{-\varepsilon_{axial}}{1 - b\varepsilon_{axial}}$$

With $E_0 = G_0 2(1+\nu)$ and $b = a\frac{\frac{2}{\sqrt{3}}(1+\nu)}{|\gamma_{0.7}|}$. solving for strain gives:

$$q = -E_0\varepsilon_{axial} + qb\varepsilon_{axial} = -(E_0 - qb)\varepsilon_{axial}$$

And

$$-\varepsilon_{axial} = \frac{1}{E_0}\frac{q}{(1 - qb/E_0)}$$

Comparing with the hyperbolic model

$$-\varepsilon_1 = \frac{1}{E_i}\frac{q}{1 - q/q_a}$$

The results are identical if $E_0 = E_i$ and $\frac{E_0}{b} = q_a$. The latter equation fully written out gives:

The Small strain model is equal to the hyperbolic model if

$$\gamma_{0.7} = \frac{q_a}{E_i}\frac{2}{\sqrt{3}}a(1+\nu)$$

$$G_0 = \frac{E_i}{2(1+\nu)}$$

In the Plaxis manual

Mohr-Coulomb failure criterion in Eqs. (7.2) and (7.3) yields:

$$\gamma_{0.7} \approx \frac{1}{9G_0}[2c'(1+\cos(2\varphi')) - \sigma'_1(1+K_0)\sin(2\varphi')] \quad (7.14)$$

where K_0 is the earth pressure coefficient at rest and σ'_1 is the effective vertical stress (pressure negative).

8 Signature

Delft, <datum>	TNO
<naam afdelingshoofd> Head of department	J.P. Pruiksma Author